IDŐJÁRÁS

Quarterly Journal of the Hungarian Meteorological Service
Vol. 117, No. 31, July–September 2013, pp. 277–294

Performance of the Asymmetric Convective Model Version 2, in the Unified EMEP Model

Zorica Podrascanin[1]* and **Dragutin T. Mihailovic** [2]

[1]*Faculty of Sciences, Department of Physics, University of Novi Sad, Dositej Obradovic Sq. 4, 21000 Novi Sad, Serbia*

[2]*Faculty of Agriculture, Department of Field and Vegetable Crops, University of Novi Sad, Dositej Obradovic Sq. 8, 21000 Novi Sad, Serbia, guto@polj.uns.ac.rs*

**Corresponding author E-mail: zorica.podrascanin@gmail.com*

(Manuscript received in final form March 6, 2013)

Abstract–We have investigated the performance of the Asymmetric Convective Model Version 2 (ACM2), a planetary boundary layer (PBL) vertical turbulent mixing scheme, that is a combination of local and non-local closures, in a complex system such as a chemical transport model, the Unified EMEP (European Monitoring and Evaluation Program) Model. For this purpose, we modified the local part of the ACM2 scheme to take into account the level of turbulent kinetic energy, and then incorporated this scheme in the Unified EMEP model. After incorporation, the scheme was validated under all stability conditions and for several compounds. Comparisons were made against the K-scheme currently used in the Unified EMEP model, and surface nitrogen dioxide (NO_2), sulfur dioxide (SO_2), and sulphate (SO_4^{2-}) concentrations were observed at different EMEP stations during the year 2005. In most cases, the model better simulated the NO_2, SO_2, and SO_4^{2-} concentrations when the ACM2 scheme was used, especially for NO_2 during the summer months, when the non-local mixing is presumably dominant.

Key-words: non-local convective mixing, local scheme, turbulent kinetic energy, chemical modeling, vertical turbulent mixing

1. Introduction

The Unified EMEP model (*Simpson et al.*, 2003) was developed as a part of the European Monitoring and Evaluation Programme (EMEP) under the Convention on Long-Range Transboundary Air Pollution (LRTAP). This and previous versions of this model have been used over the last 30 years to simulate the transboundary transport of air pollution on the European scale. The surface concentrations of pollutants are strongly related to the turbulent vertical mixing, and thus, a good representation of vertical mixing in the planetary boundary layer (PBL) is very important for every chemical transport model, including the Unified EMEP model. During the past 30–50 years, various turbulent vertical mixing schemes for use in the PBL were developed and tested in 1D and 3D simulations in both meteorological and air quality models. All of the suggested vertical mixing schemes can be categorized as diffusion schemes, K-schemes (e.g., *O'Brien*, 1970; *Deardorff*, 1972; *Louis*, 1979; *Holtslag* and *Moeng*, 1991; *Holtslag* and *Boville*, 1993; *Alapaty* and *Alapaty*, 2001), second and higher-order closure models (e.g., *Mellor* and *Yamada*, 1974; *Janjic*, 1990, 1994, etc.), non-local schemes (e.g., *Blackadar*, 1976; *Stull*, 1984; *Pleim* and *Chang*, 1992; *Hong* and *Pan*, 1996), and combinations of local (diffusion) and non-local schemes (e.g., *Pleim*, 2007a). Most of these schemes have been intensively tested and compared with each other and against measurements in many studies (e.g., *Zhang* and *Zheng*, 2004; *Berg* and *Zhong*, 2005; *Hu et al.*, 2010). The most important conclusions from those studies are as follows: 1) the model is sensitive to the turbulent vertical mixing scheme in the PBL; 2) the non-local aspect of these schemes is important for realistically representing the convective boundary layer (CBL); and 3) the realistic apportionment of fluxes between local and non-local components is critical for satisfactorily representing the mixing in a CBL.

The Unified EMEP model is an off-line chemical transport model, which means that the model is driven with outputs from meteorological weather prediction models without feedback between chemical and meteorological models. The advantage of this approach is the possibility of independent parameterizations, a more flexible grid construction, and that it is easier to use for the inverse modeling, among others (*Baklanov* and *Korsholm*, 2007). The Unified EMEP model uses K-schemes for parameterizing the vertical mixing: the O'Brien (*O'Brien*, 1970) scheme is used in the CBL, and the Blackadar scheme (*Blackadar*, 1979) is used in the stable boundary layer (SBL). During the past several years, some other vertical mixing schemes have been proposed for use in this model. *Mihailovic* and *Alapaty* (2007) proposed a closure based on turbulent kinetic energy (TKE) as an improvement of the vertical diffusion scheme by *Alapaty* (2003). They examined the performance of the scheme comparing simulated and measured NO_2 gas concentrations for the years 1999, 2001, and 2002. In 2008, the non-local convective mixing scheme with varying

upward mixing rates (VUR) was proposed for use in the Unified EMEP model (*Mihailovic et al.*, 2008) and was later combined with TKE vertical diffusion scheme (*Mihailovic et al.*, 2009). This combination of the two previous schemes uses the VUR scheme for convective conditions and the TKE scheme for stable conditions. The disadvantage of this approach is an abrupt change from one scheme to another in the transition from convective to stable conditions. Additionally, in the VUR schemes, bottom-up fluxes originated in the first layer are distributed to the layers above; this is not realistic, because there is clearly an additional mixing between adjacent layers. The scheme that avoids the aforementioned drawback of the previous schemes used in the EMEP model has a realistic apportionment of fluxes between the local and non-local components as a result of combined local and non-local closures; this scheme is called the Asymmetric Convective Model Version 2 (ACM2) (*Pleim*, 2007a). The ACM2 scheme is built on the original Asymmetric Convective Model (ACM) (*Pleim* and *Chang*, 1992), a non-local convective mixing scheme, by adding an eddy diffusion component. The main advantage of this scheme in comparison to the ACM scheme (which is applicable only in convective conditions) is its applicability for all stability conditions. Mixing between a non-local and local diffusion scheme, in the case of convection, is governed by a pre-specified weighting factor that depends on the PBL height and Monin-Obukhov length. In stable conditions, stratification mixing is reduced to local diffusion. The ACM2 scheme has been tested in its 1D form against large-eddy simulations (LES) (*Pleim*, 2007a) and has been implemented in the meteorological model (fifth-generation Pennsylvania State University–NCAR Mesoscale Model (MM5)) (*Pleim*, 2007b). The profiles obtained with the ACM2 scheme in the 1D test have shapes that are more similar to the shapes of the LES profiles than those obtained with the ACM scheme. The MM5 model with the ACM2 scheme is evaluated with surface meteorological measurements, rawinsonde profile measurements, and the observed PBL height. The MM5 model with ACM2 performed as well or better than similar MM5 model studies.

We have incorporated the ACM2 scheme into the Unified EMEP model because of its previously mentioned properties to test its ability to work in a complex system that depends on a large number of processes: horizontal advection, emissions, vertical mixing, chemical reactions, dry and wet deposition, among others. For this purpose, we modified the local part of ACM2 to account for the level of turbulent kinetic energy and then incorporated it in the Unified EMEP model. The goal of this study was to demonstrate the possibility of applying the ACM2 scheme in the Unified EMEP model on the most important air pollutants from an environmental standpoint: NO_2, SO_2, and SO_4^{2-} (*Jericevic et al.*, 2010). The validation has been performed for all stability conditions, and the modeled surface nitrogen dioxide (NO_2), sulfur dioxide (SO_2), and sulphate (SO_4^{2-}) concentrations were compared with observations at different EMEP measurement stations during the year 2005. Descriptions of the

standard Unified EMEP schemes and the ACM2 scheme are given in Section 2. The comparison results between the currently used scheme in the Unified EMEP model, the ACM2 scheme, and the measured concentrations are given in Section 3, while Section 4 summarizes the study and presents the concluding remarks.

2. Materials and methods

2.1. Formulation of the vertical diffusion currently used in the Unified EMEP chemical model

The vertical sub-grid transport is modeled using the K-scheme in the Unified EMEP chemical model as well as in many other chemical transport models. K is determined in the unstable conditions as

$$K(z)=\begin{cases} K(h)+\left(\dfrac{h-z}{h-h_s}\right)^2\left\{\left[K(h_s)-K(h)\right]+\right. \\ \qquad \left.(z-h_s)\left[\dfrac{\delta}{\delta_s}K(h_s)+2\dfrac{K(h_s)-K(h)}{h-h_s}\right]\right\}, & h_s \le z < h \\ \dfrac{u_* kz}{\phi\left(\dfrac{z}{L}\right)}, & z < h_s \end{cases} \tag{1}$$

where z is the model layer height, h is the PBL height, h_s is the surface boundary layer height, u_* is friction velocity, ϕ is the atmospheric stability function for temperature, and k is the von Karman constant. In the model calculation, h_s is equal to 4% of the PBL height (*O'Brien*, 1970). The atmospheric stability function for temperature in convective conditions is

$$\phi=\left(1-16\frac{z}{L}\right) \tag{2}$$

and for stable conditions is

$$\phi=1+5\frac{z}{L}. \tag{3}$$

Accordingly, K is calculated in stable conditions and above the PBL (*Blackadar*, 1979) as

$$K(z)=\begin{cases}0.001 & R_{\mathrm{i}} > R_{ic} \\ 1.1(R_{\mathrm{ic}}-R_i)l^2\left|\Delta V_{\mathrm{H}}/\Delta z\right|R_{\mathrm{ic}} & R_i \le R_{ic}\end{cases}, \tag{4}$$

where l is the turbulent mixing length, ΔV_{H} represents the difference in wind-speed between two grid-cell centers separated by distance Δz, R_i is the Richardson number and R_{ic} is the critical Richardson number. The turbulent mixing length is parameterized according to:

$$\begin{aligned} l &= kz, \quad z \le z_m \\ l &= kz_m, \quad z > z_m \end{aligned} \tag{5}$$

where k is the von Karman constant, z is the height above the ground, and $z_m = 200$ m. Hereafter, the currently used scheme in the Unified EMEP model will be called the OLD scheme.

2.2. Formulation of the ACM2 scheme for use in the Unified EMEP model

According to the ACM2 scheme, the quantity φ in the model layer i is calculated as

$$\frac{\partial \varphi_i}{\partial t} = Mu'\varphi_1 - Md'_i\varphi_i + Md'_{i+1}\varphi_{i+1}\frac{\Delta z_{i+1}}{\Delta z_i} + \frac{1}{\Delta z_i}\left[\frac{K'_{i+1/2}(\varphi_{i+1}-\varphi_i)}{\Delta z_{i+1/2}} - \frac{K'_{i-1/2}(\varphi_i-\varphi_{i-1})}{\Delta z_{i-1/2}}\right], \tag{6}$$

where Mu' and K' are the upward convective mixing rate and a diffusion coefficient, respectively, weighted by the factor f_{conv}, and Δz_i is the thickness of layer i. This factor f_{conv} controls the degree of local versus non-local behavior. The scheme reverts to either the non-local or local scheme for $f_{conv}=1$ or $f_{conv}=0$, respectively. The f_{conv} is estimated as

$$f_{conv} = \left[1+\frac{k^{-2/3}}{0.1a}\left(-\frac{h}{L}\right)^{-1/3}\right]^{-1}, \tag{7}$$

where k is the von Karman constant, h is the PBL height, L is the Monin-Obukhov length, and a is set to 7.2. The Mu', Md' and K' were calculated as

$$Mu' = \frac{f_{conv}K(z_{1+1/2})}{\Delta z_{1+1/2}(h-z_{1+1/2})}, \tag{8}$$

$$Md_i' = \frac{Mu'(h - z_{i-1/2})}{\Delta z_i} \tag{9}$$

and

$$K'(z) = K(z)(1 - f_{conv}), \tag{10}$$

where z is the height of the model layer and h is the PBL height. The diffusion coefficient K is calculated as in *Mihailovic* and *Alapaty* (2007). This method was chosen because it takes into account the level of TKE, which is a decisive parameter in the vertical mixing within the PBL. In the PBL, K is calculated as

$$K(z) = \frac{\bar{e}_* kz\left(1 - \frac{z}{h}\right)^2}{\phi}, \tag{11}$$

where $\bar{e}_*$ is the mean turbulent velocity scale within the PBL, k is the von Karman constant, z is the vertical coordinate, h is the PBL height, and ϕ is the atmospheric stability function for temperature (Eqs. (2-3)). The mean turbulent velocity scale within the PBL is calculated as

$$\bar{e}_* = \frac{1}{h}\int_0^h \sqrt{e(z)}\Psi(z)\,dz, \tag{12}$$

where Ψ is the vertical profile function (see *Mihailovic* and *Alapaty* (2007) for details about this function) and e is TKE.

The TKE vertical profile, $e(z)$, for near neutral to free convection conditions (*Zhang et al.*, 1996) is expressed as

$$e(z) = \frac{1}{2}\left(\frac{L_E}{h}\right)^{\frac{2}{3}}\left(0.4w_*^3 + u_*^3(h - z)\frac{\phi}{kz}\right)^{\frac{2}{3}}, \tag{13}$$

where h is the PBL height, $L_E = 2.6h$, w_* is the convective velocity scale, u_* is the friction velocity scale, k is the von Karman constant, and ϕ is a non-dimensional function of heat. For the stable atmospheric boundary layer, we modeled the TKE profile using an empirical function (*Lenschow et al.*, 1988) based on aircraft observations:

$$e(z) = 6u_*\left(1 - \frac{z}{h}\right)^{1.75}, \tag{14}$$

where h is the PBL height, z is the height of the model layer, and u_* is the friction velocity scale. Above the PBL, the diffusion coefficient K is calculated using Eq. (4).

2.3. Short description and model setups

The EMEP chemical model is designed to describe the transboundary acidification, eutrophication, and ground level ozone in Europe and has influenced European air quality policies since the late 1970s. Since the 1990s, this model has provided the reference inputs for the integrated assessment modeling atmospheric dispersion calculations. The Unified EMEP chemical model was developed at the Norwegian Meteorological Institute. In this work, tests were performed using the rv3.0 version of this model (*Simpson et al*., 2003). The model advection is designed using a scheme by *Bott* (1989a, 1989b); the diffusion scheme, which is described in Section 2.1, is used for the turbulent vertical mixing. The Unified EMEP chemical model emissions inputs are provided for 10 anthropogenic source sectors and consist of gridded annual national emissions of sulfur dioxide (SO2), nitrogen oxides (NOx = NO + NO2), ammonia (NH3), non-ethane volatile organic compounds (NMVOC), carbon monoxide (CO), and particulates (PM2.5, PM10). The meteorological fields used in the model are provided every 3 hours from PARLAM-PS, which is a dedicated version of the HIRLAM (High Resolution Limited Area Model) Numerical Weather Prediction (NWP) model with parallel architecture (*Bjorge* and *Skalin*, 1995; *Berge* and *Jakobsen*, 1998; *Lenschow* and *Tsyro*, 2000). The linearly interpolated 3-hour meteorological fields, wind components, temperature and humidity, cloudiness, precipitation, and momentum and energy fluxes between the surface and atmosphere are then used to calculate the velocity scales, PBL height, and Monin-Obukhov length in every model time step. Note that we calculate new mixing levels using meteorological parameters from the meteorological model that has its own mixing. The parameters imported from PARLAM-PC are the friction velocity and energy fluxes. These parameters come from the Monin-Obukhov theory, that has been widely accepted as the best theory for the surface layer with the implicit assumption that the rest of the PBL mixing should be improved. The Unified EMEP model uses a polar-stereographic projection, true at 60° N, with a grid size of 50×50 km^2 and a vertical σ coordinate with 20 levels. The horizontal grid of the model is the Arakawa C grid. All other model details can be found in *Simpson et al.* (2003). The domain with (131, 100) points is used in the simulations with a 1200 s time step and with the 3-hour resolution meteorological data from the PARLAM-PS model.

2.4. EMEP measurement network

The EMEP measurement network was one of the first international environmental measurement networks established in Europe. The data sets from that network are

well documented, quality controlled, and suitable for comparing with model results. All details on measurement techniques, location of stations, and data sets can be found at http://www.nilu.no/projects/ccc/emepdata.html. The observed values from the EMEP measurement network have already been used in many papers for testing various mixing schemes as well as for other chemical transport studies (*Topçu et al.*, 2002; *Mihailovic* and *Alapaty*, 2007; *Mihailovic et al.*, 2009; *Calvo et al.*, 2010). In this study, we analyze the influence of the ACM2 scheme for vertical mixing in the PBL on the quality of the model's performance. For comparison, we have chosen the year 2005 and compared our results against surface concentration measurements of NO_2 ($\mu g\,N\,m^{-3}$), SO_2 ($\mu g\,S\,m^{-3}$), and SO_4^{2-} ($\mu g\,S\,m^{-3}$) from the EMEP stations because of their good spatial and temporal resolutions. Furthermore, these three compounds were chosen because they are important acidifying and atrophying pollutants and play a significant role in air pollution in Europe. Nitrogen contributes to the formation of photochemical smog, which can have significant impacts on human health. Sulphate, an oxidant of SO_2, is a secondary pollutant that contributes to acid rain formation. Mixing in the lower part of the PBL will influence mostly those tracers that have sources on the ground. This is not the case with ozone, the daytime concentration of which is primarily controlled by photochemistry and transport rather than the vertical mixing; therefore, the interpretation of the influence of vertical mixing on ozone concentrations is much more difficult (*Pleim*, 1992). Note that the Unified EMEP chemical model outputs cannot be always compared with observations in this network because of the coarse horizontal model resolution, which is especially pronounced at high altitudes. Additionally, a problem is encountered with the shipping emission path, because the high concentrations are horizontally diffused over a large area. The differences between the observed and modeled concentrations might be due to other reasons, such as stations can be affected by local sources, emissions, meteorology, and chemistry, among others. Some mountain stations (e.g., SK002R, DE003R, PL003R, and DE008) and some stations in the North Sea shipping area (e.g., DK005R, DE008R, and EE011R) with the highest discrepancies were excluded from the comparison (*Jericevic et al.*, 2010).

3. The results and discussion

The Unified EMEP model Version rv3.0 was first run with the OLD scheme with the setup described in Section 2.3. Whenever a new scheme is introduced into a model, the first step in the analysis usually concerns the differences between the new and the old vertical mixing schemes, especially for the chemical species that originate in the ground. At this moment, the full importance of comparing with the OLD scheme becomes evident. If just one aspect of the model is changed and the result improves, then it is very likely that the introduced change was the

reason for the improvement. Clearly, this may not be always true in a complex meteorological-chemistry model. Then, if there is some sensitivity to introducing a new scheme, the model results are compared with the measurements if they are available. Eventually, better results with the new scheme suggest that it should be used in the Unified EMEP model. In our analysis, we will concentrate on the monthly averaged value of concentrations for the four aforementioned compounds. However, to be absolutely sure that a scheme is stable and that the monthly averaged value of concentrations is not a consequence of very low or very high peaks in daily concentrations, it is necessary to evaluate the daily concentrations in this scheme.

In addition to monthly averages, we will also present some diurnal variations as well as annual averages. For that purpose, we will use a few stations from the EMEP measurement network that are at different locations and altitudes. Station AT0002R is a measurement site located in Illmitz, Austria, at 47º 46'N, 16º 46'E and at an altitude of 117 m above sea level; station DE0001R is a measurement site located in Westerland, Germany, at 54º 56'N, 08º 19'E and at an altitude of 10 m above sea level; the station CZ0001R is a measurement site located in Svratouch, Czech Republic, at 49º 44'N, 16º 02'E and at an altitude of 737 m above sea level; station FR0012R is a measurement site located in Iraty, France, at 43º 02'N, 01º 05'W and at an altitude of 1300 m above sea level; and station DE0007R is a measurement site located in Neuglobsow, Germany, at 53º 09'N, 13º 02'E and at an altitude of 62 m above sea level. The annual time series of daily NO_2 and SO_2 concentrations at the stations AT0002R, DE0001R, and CZ0001R are depicted in *Fig. 1* and *2*, respectively, while the daily SO_4^{2-} concentrations at the stations FR0012R, DE0007R, and CZ0001R are shown in *Fig. 3*. The surface concentrations of NO_2 obtained by the ACM2 scheme at all stations are higher than those obtained with the OLD scheme. The differences between the concentrations of SO_2 and SO_4^{2-} obtained with the ACM2 and OLD schemes are not as pronounced as with the NO_2 concentrations. The root mean square error (RMSE) and mean annual concentration (MAC) for the above-mentioned stations are shown in *Tables 1-3* for the concentrations of NO_2, SO_2, and SO_4^{2-}, respectively. The RMSE values for the NO_2 concentrations are lower when the ACM2 scheme was used at the stations AT0002R and CZ0001R and higher for station DE0001R. The mean annual concentrations of NO_2 obtained by the ACM2 scheme at all stations are closer to the measured mean annual concentrations. The RMSE and MAC values obtained with the OLD and ACM2 schemes are very similar for the concentrations of SO_2 and SO_4^{2-}. The scatter plot diagrams with coefficient of determination (R^2) between measured and modeled concentrations with the OLD and ACM2 schemes for NO_2, SO_2, and SO_4^{2-} at mentioned stations are showed in *Fig. 4*. The R^2 between daily measured and modeled data is slightly higher when the ACM2 scheme is used than the OLD scheme for the concentrations of NO_2 and SO_2 and opposite for the concentration of SO_4^{2-}.

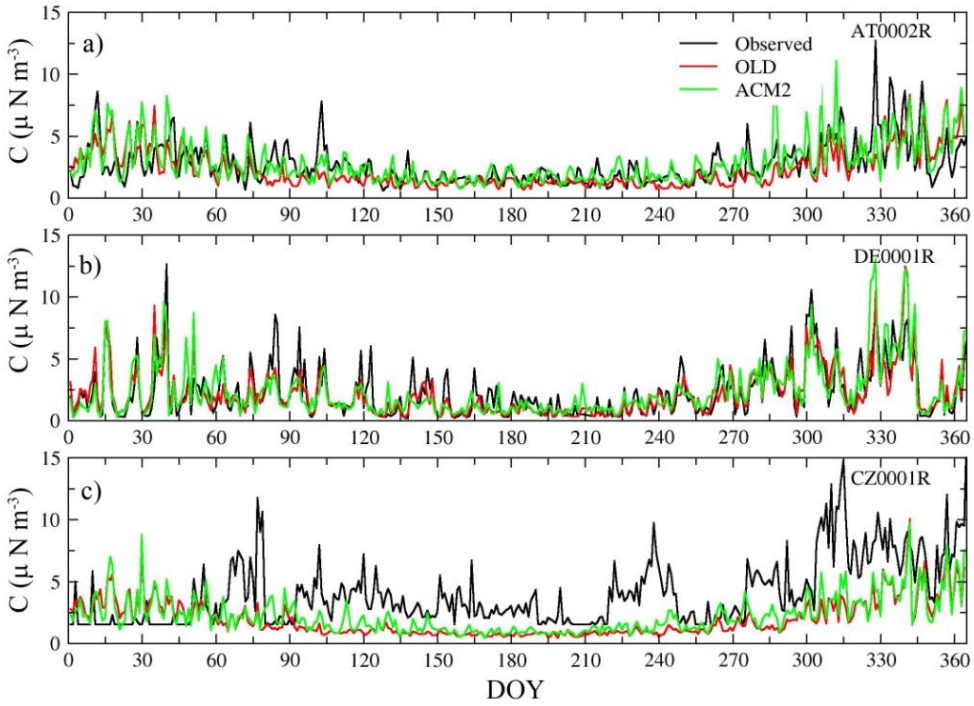

Fig. 1. Time series of the measured and modeled daily surface NO2 concentrations for a) AT0002R, b) DE0001R, and c) CZ0001R in the year 2005. Modeled results are obtained with two vertical diffusion schemes: OLD and ACM2. The time is shown on the x-axis as the day of the year (DOY).

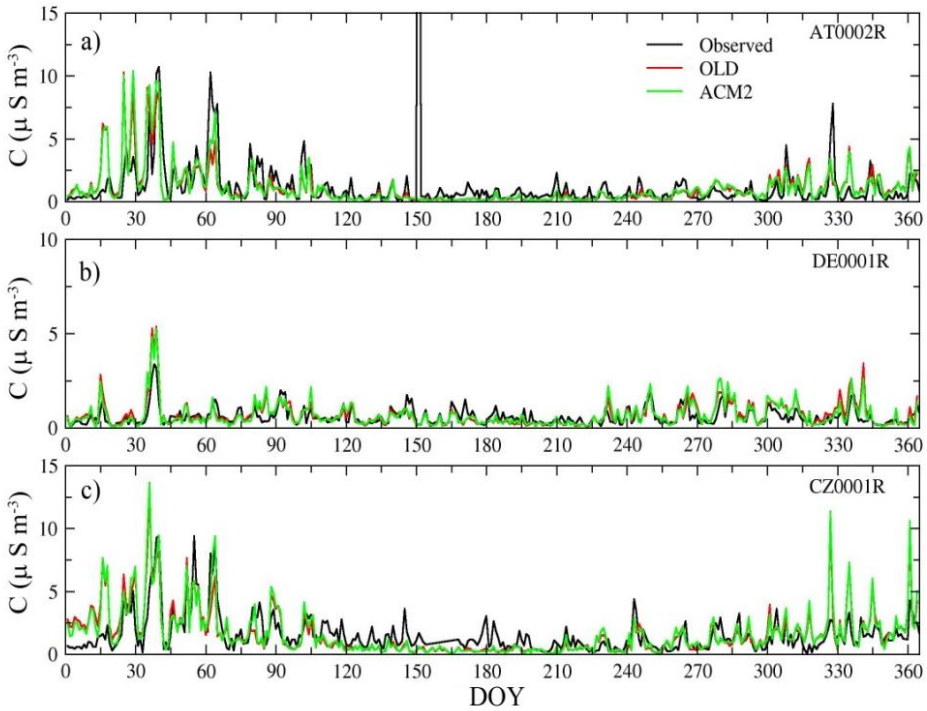

Fig. 2. Time series of the measured and modeled daily surface SO2 concentrations for a) AT0002R, b) DE0001R, and c) CZ0001R in the year 2005. The modeled results are obtained with two vertical diffusion schemes: OLD and ACM2. The time is shown on the x-axis as the day of the year (DOY).

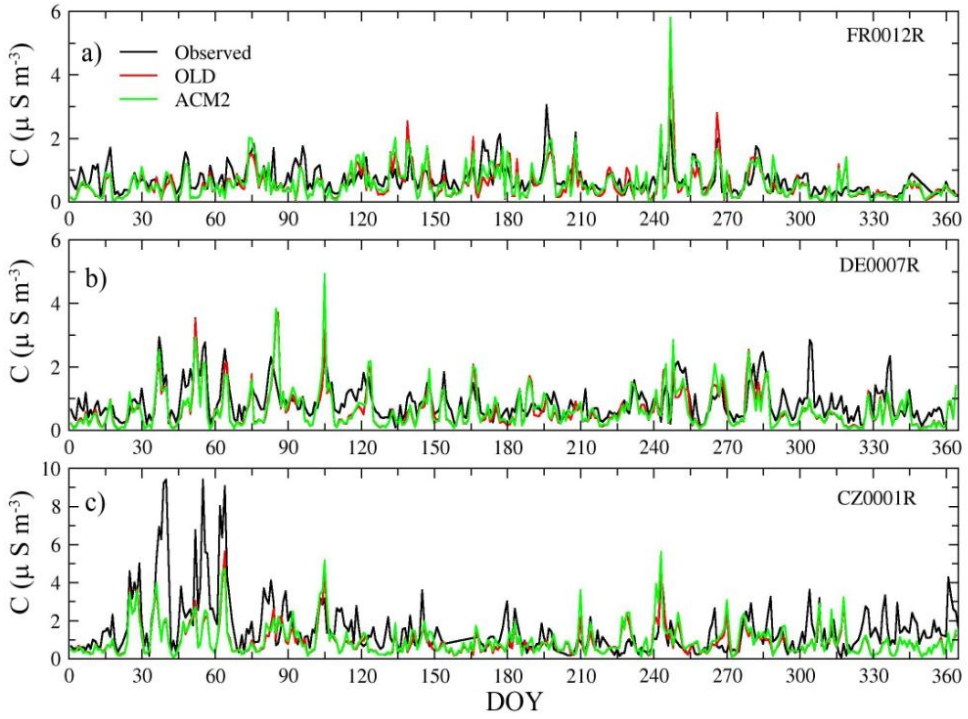

Fig. 3. Time series of the measured and modeled daily surface SO_4^{2-} concentrations for a) FR0012R, b) DE0007R, and c) CZ0001R in the year 2005. Modeled results are obtained with two different vertical diffusion schemes: OLD and ACM2. The time is shown on the x-axis as the day of the year (DOY).

Table 1. RMSE and mean annual concentration of NO_2

Station	**RMSE (OLD)**	**RMSE (ACM2)**	**MAC(OLD) (μg N m^{-3})**	**MAC(ACM2) (μg N m^{-3})**	**MAC (observed) (μg N m^{-3})**
AT0002R	1.66	1.59	2.26	2.82	2.69
DE0001R	1.30	1.52	2.16	2.33	2.33
CZ0001R	3.21	2.96	1.91	2.23	4.00

Table 2. RMSE and mean annual concentration of SO_2

Station	**RMSE (OLD)**	**RMSE (ACM2)**	**MAC(OLD) (μg S m^{-3})**	**MAC(ACM2) (μg S m^{-3})**	**MAC(observed) (μg S m^{-3})**
AT0002R	3.45	3.45	1.05	1.09	1.25
DE0001R	0.45	0.44	0.70	0.67	0.59
CZ0001R	1.43	1.47	1.56	1.67	1.72

Table 3. RMSE and mean annual concentration of SO_4^{2-}

Station	RMSE (OLD)	RMSE (ACM2)	MAC(OLD) (μg S m^{-3})	MAC(ACM2) (μg S m^{-3})	MAC (observed) (μg S m^{-3})
FR0012R	0.43	0.43	0.56	0.58	0.70
DE0007R	0.49	0.52	0.62	0.63	0.88
CZ0001R	1.37	1.39	0.92	1.00	1.56

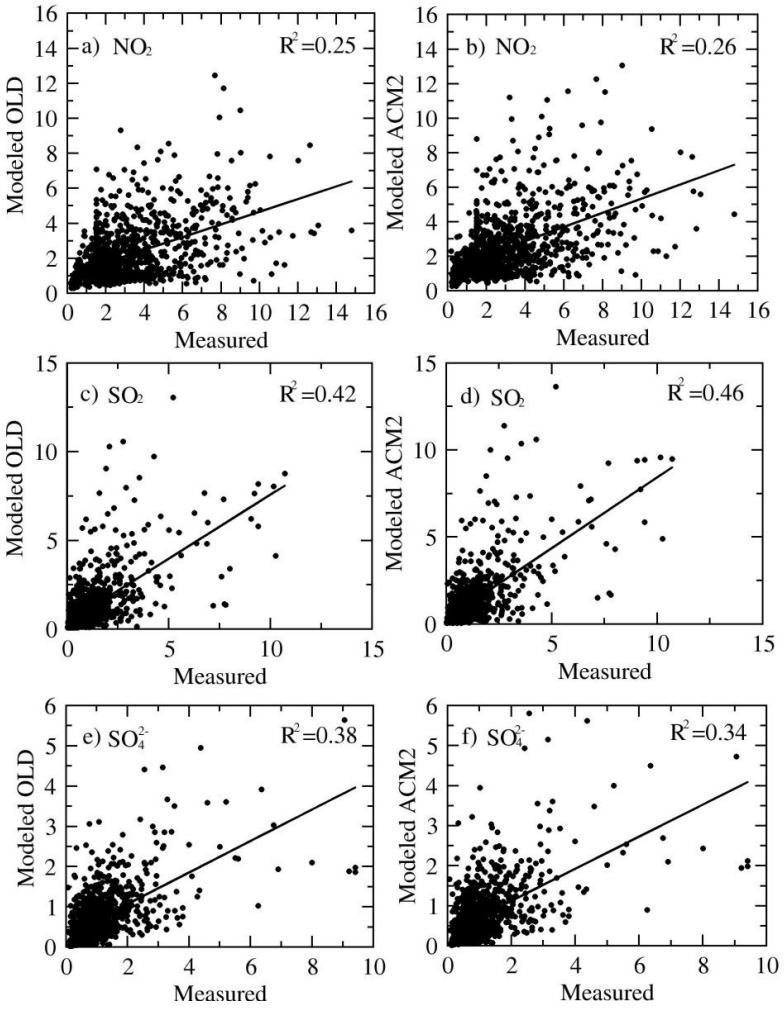

Fig. 4. Scatter plot diagrams of modeled against measured daily concentrations with corresponding coefficients of determination. Panels are: concentration of NO2 modeled by a) OLD and b) ACM2; concentration of SO2 modeled by c) OLD and d) ACM2, and concentration of SO_4^{2-} modeled by e) OLD and f) ACM2.

After the analysis of the daily concentrations showed that there are no peaks in this concentration, we compared the average monthly concentrations at the stations from the EMEP network, except those mentioned in Section 2.4 with the model results obtained using the OLD and ACM2 schemes. The scatter plot

diagrams with R^2 between monthly concentrations of NO_2, SO_2, and SO_4^{2-} calculated using the OLD and ACM2 scheme and corresponding measured concentrations are depicted in *Fig. 5*. The R^2 between monthly measured and modeled data using the OLD and ACM2 scheme are very similar for all compounds. To compare the results, we calculated the following statistical quantities: (i) RMSE, (ii) BIAS, and (iii) standard deviations of the simulations (SDS) and observations (SDO). These quantities are given by the following equations:

$$\mathrm{RMSE} = [\sum_{i=1}^{N_s} (M_i - O_i)^2 / N_s]^{1/2} , \quad (15)$$

$$\mathrm{BIAS} = \left(\frac{\overline{M} - \overline{O}}{\overline{O}} \right) \cdot 100\% , \quad (16)$$

$$\mathrm{SDS} = [\sum_{i=1}^{N_s} (M_i - \overline{M})^2 / N_s]^{1/2} , \quad (17)$$

$$\mathrm{SDO} = [\sum_{i=1}^{N_s} (O_i - \overline{O})^2 / N_s]^{1/2} , \quad (18)$$

where M_i and O_i denote the modeled and observed average monthly concentrations, respectively, and N_s is the number of stations, while an over bar indicates an average monthly concentration for all stations.

Biases for the measured and modeled average monthly NO_2, SO_2, and SO_4^{2-} concentrations for both schemes are shown in *Fig. 6*. In the upper panel of this figure, the BIAS of the ACM2 scheme is observed to be lower than that of the OLD scheme. Both schemes underestimate the observations during the warmer months, but the ACM2 scheme overestimates the observed NO_2 concentration in the colder months. Inspecting the BIAS for SO_2 (middle panels of the same figure) does not show larger differences in the BIAS for the OLD and ACM2 schemes. Both schemes underestimate the SO_2 observations during the warmer months and overestimate them during the colder months. The BIAS of the ACM2 scheme for SO_4^{2-} (lower panels of the same figure) is lower than for the OLD schemes. Both schemes underestimate the SO_4^{2-} observations except for September, when the ACM2 scheme overestimates the observations. The higher BIAS obtained for SO_4^{2-} may be due to many complicated processes, including microphysics and aqueous phase reactions, connected with this particular compound. Our understanding of *Fig. 6* is as follows: in the colder part of the year, the atmosphere is basically stable; therefore, the diffusive part of the ACM2 scheme has a greater contribution to its

performance. In contrast to the colder months, the warmer months are more influenced by the non-local part of the ACM2 scheme. The smaller BIAS between the modeled and observed concentrations for the ACM2 scheme indicates that the average estimated concentrations are closer to the average observed concentrations.

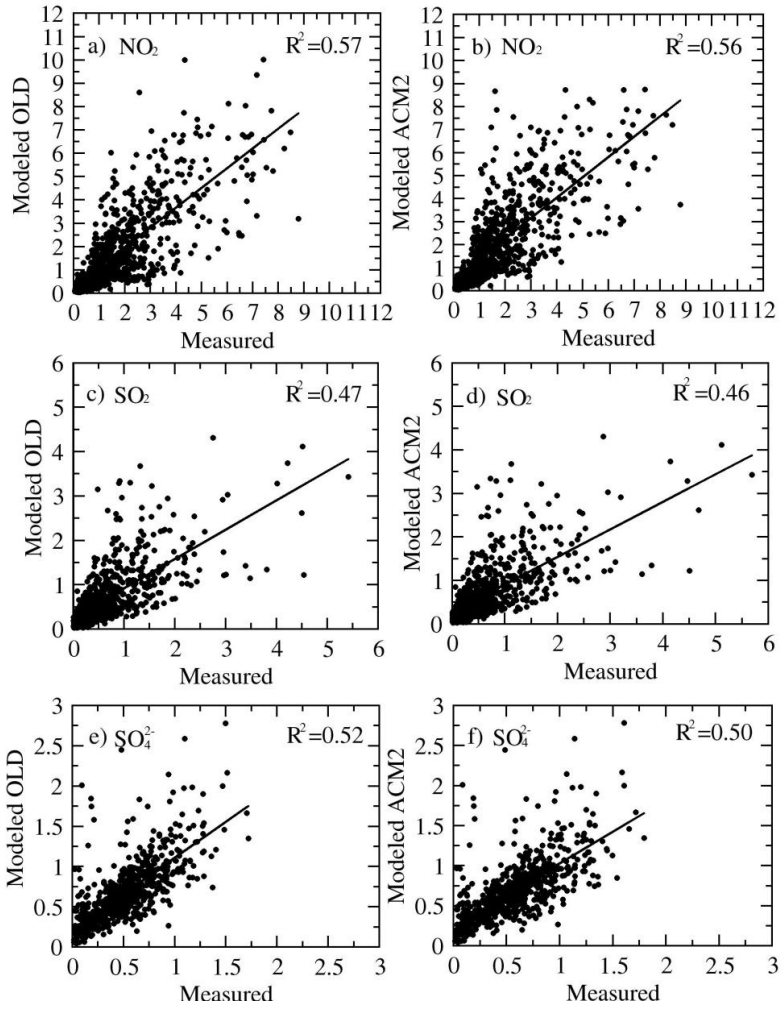

Fig. 5. Scatter plot diagrams of modeled against measured monthly concentrations with corresponding coefficients of determination. Panels are: concentration of NO2 modeled by a) OLD and b) ACM2; concentration of SO2 modeled by c) OLD and d) ACM2, and concentration of SO_4^{2-} modeled by e) OLD and f) ACM2.

The RMSE is a good measure in this type of comparison, and *Fig. 7* shows the RMSE for the measured and modeled average monthly NO_2, SO_2, and SO_4^{2-} concentrations for both schemes. In the upper panel of this figure, the RMSE of the ACM2 scheme is shown to be slightly lower than that for the OLD scheme, except January and December. A further inspection of the RMSE for SO_2 and SO_4^{2-} (middle and lower panels of the same figure) shows that the non-local scheme and the OLD scheme show similar behavior, i.e., SO_2 and SO_4^{2-} are very similar.

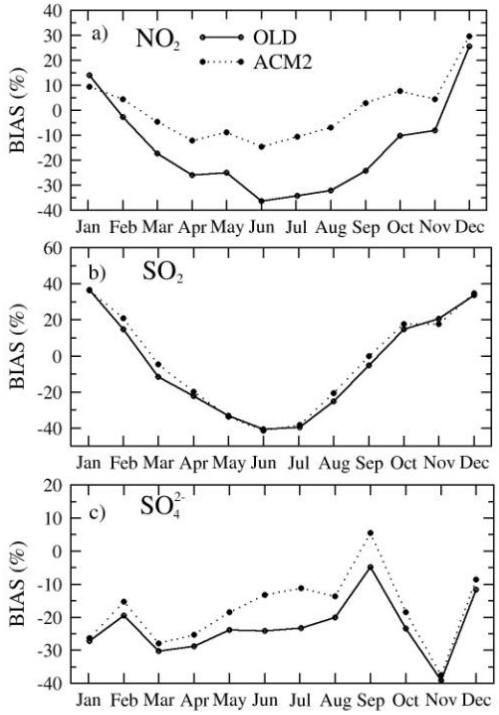

Fig. 6. Average monthly BIAS (%) for the observed and modeled (a) NO_2, (b) SO_2 and (c) SO_4^{2-} concentrations for the ACM2 and OLD schemes used in the Unified EMEP chemical model for 2005.

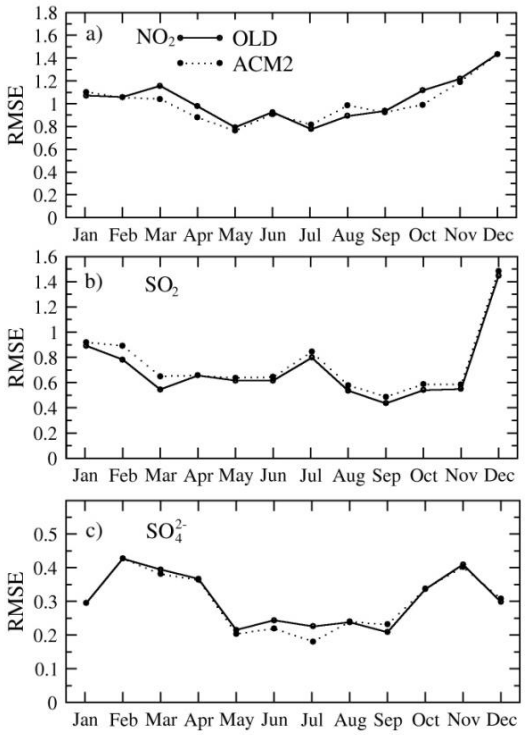

Fig. 7. Average monthly RMSE values for the observed and modeled concentrations of (a) NO2, (b) SO2, and (c) SO_4^{2-} for the ACM2 and OLD schemes used in the Unified EMEP chemical model for 2005.

The final statistics compared are the standard deviations of the observed and modeled concentrations. The standard deviations of the average monthly observed and modeled concentrations (SDS and SDO), given by Eqs. (17)–(18), are depicted in *Fig. 8*. The scheme is considered to give better results if its SDS is closer to its SDO. It can be concluded from this figure that (i) the SDS for both schemes are higher for colder months except for SO_4^{2-}, and that (ii) the SDS for the ACM2 scheme is much closer to the SO_4^{2-} SDO. For both schemes, the SDS values are similar for some months, indicating that they have the same yearly pattern.

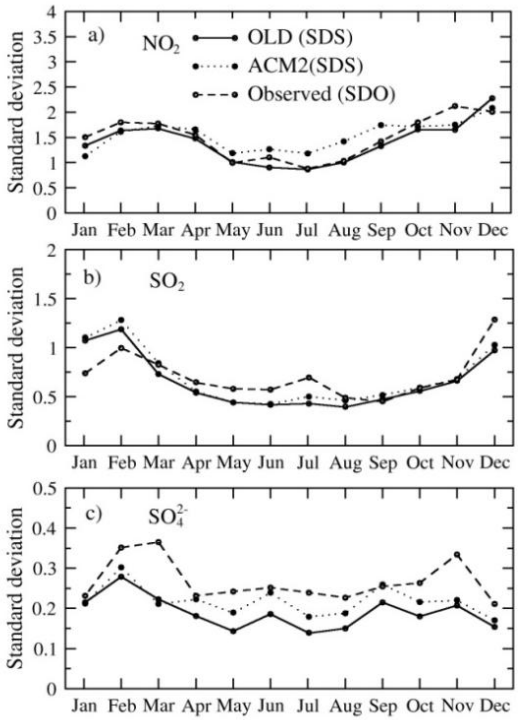

Fig. 8. Average monthly SDO and SDS values of (a) NO_2, (b) SO_2, and (c) SO_4^{2-} for the ACM2 and OLD schemes used in the Unified EMEP chemical model for 2005.

4. Conclusions

The ACM2 scheme was incorporated into a Unified EMEP model. Comparisons between the already present scheme and the new one were made, and sensitivity was demonstrated. Furthermore, the outputs of NO_2, SO_2, and SO_4^{2-} surface concentrations for both schemes were compared with the measured values. In most cases, it was shown that the Unified EMEP chemical model slightly better simulates the concentrations of NO_2, SO_2, and SO_4^{2-} when the ACM2 scheme is used. The sensitivity of the NO_2 concentrations to the choice of vertical scheme is much higher than for the other analyzed compounds. The lifetime of NO_2 in troposphere is short and has a seasonal variability. It is the shortest during the

summer months. Additionally, during the summer months the mixing driven by bouncy is fast. Those are the reasons why the sensitivity of the NO_2 concentrations to the choice of vertical scheme is much higher than for the other analyzed compounds, and it is particularly emphasized for their concentrations during the summer months. Let us note that the lifetime of both compounds, SO_2 and SO_4^{2-} is longer than that of NO_2, so it is more influenced by the horizontal advection than by vertical mixing. Overall, the agreement with the measured values is reasonably good, such that the ACM2 scheme could be used in the Unified EMEP model. Furthermore, as the ACM2 scheme possesses a higher level of sophistication, it is expected that its influence will be higher with the increased horizontal resolution of the Unified EMEP model.

Acknowledgements–This paper was realized as a part of the project "Studying climate change and its influence on the environment: impacts, adaptation and mitigation" (No. III43007), which is financed by the Ministry of Education and Science of the Republic of Serbia within the framework of integrated and interdisciplinary research over the period 2011-2014. The authors would like to thank the Norwegian Meteorological Institute for giving us the meteorology inputs for the Unified EMEP chemical model for 2005.

References

Alapaty, K., 2003: Development of two CBL schemes using the turbulence velocity scale. Proceedings of 4thWRF Users' workshop, Boulder (http://www.wrf-model.org/wrfadmin/presentations.php).

Alapaty, K. and *Alapaty, M.*, 2001: Evaluation of a nonlocal-closure K-scheme using the MM5. Workshop Program for the Eleventh PSU/NCAR MM5 Users' Workshop, Foothills Laboratory, NCAR (http://www.mmm.ucar.edu/mm5/workshop/).

Baklanov, A. and *Korsholm, U.*, 2007: On-line integrated meteorological and chemical transport modeling: Advantages and Prospectives. In (Eds.: *Borrego, C.* and *Miranda, A.I.*) Proceedings of the 29th NATO/CCMS International Technical Meeting on Air pollution Modelling and its Application, 24–28 September 2007, Aveiro.

Berg, L.K. and *Zhong, S.*, 2005: Sensitivity of MM5-simulated boundary layer characteristics to turbulence parameterizations. *J. Appl. Meteor. 44*, 1467–1483.

Berge, E. and *Jakobsen, H.A.*, 1998: A regional scale multi-layer model for the calculation of long-term transport and deposition of air pollution in Europe. *Tellus 50*, 205–223.

Bjorge, D. and *Skalin, R.*, 1995: PARLAM – the parallel HIRLAM version at DNMI. Research Report, No.27, Norwegian Meteorological Institute, Oslo.

Blackadar, A.K., 1976: Modeling the nocturnal boundary layer. Preprints, 3rd Symposium on Atmospheric Turbulence, Diffusion and Air Quality, Raleigh, NC, 19–22 October 1976, *Amer. Meteor. Soc.*, 46–49.

Blackadar, A.K., 1979: High resolution models of the planetary boundary layer. In (Eds. Pfaffin, J.R., and Ziegler, E.N.) Advances in environment and scientific engineering, Vol. 1, Gordon and Breach, Newark, 50–85.

Bott, A., 1989a: A positive definite advection scheme obtained by non-linear re-normalization of the advection uses. *Mon. Weather Rev. 117*, 1006–1015.

Bott, A., 1989b: Reply. *Mon. Weather Rev. 117*, 2633–2636.

Calvo, A.I., Olmo, F.J., Lyamani, H., Alados-Arboledas, L., Castro, A., Fernández-Raga, M., and *Fraile, R.*, 2010: Chemical composition of wet precipitation at the background EMEP station in Víznar (Granada, Spain) (2002–2006). *Atmos. Res. 96*, 408–420.

Deardorff, J.W., 1972: Theoretical expression for the countergradient vertical heat flux, *J. Geophys. Res. 77(30)*, 5900–5904.

Holtslag, A.A.M., and *Boville, B.A.,* 1993: Local versus nonlocal boundary-layer diffusion in a global climate model. *J. Climate 6*, 1825–1842.

Holtslag, A.A.M., and *Moeng, C.-H.,* 1991: Eddy diffusivity and countergradient transport in the convective atmospheric boundary layer. *J. Atmos. Sci. 48*, 1690–1698.

Hong, S.Y., and *Pan, H.L.,* 1996: Nonlocal boundary layer vertical diffusion in a Medium-Range Forecast model. *Mon. Weather Rev. 124*, 2322–2339.

Hu, X.-M., Nielsen-Gammon, J.W., and *Zhang, F.,* 2010: Evaluation of three planetary boundary layer schemes in the WRF model. *J. Appl. Meteor. Climatol. 49*, 1831–1844.

Janjic, Z.I., 1990: The step-mountain coordinate: Physical package. *Mon. Weather Rev. 118*, 1429–1443.

Janjic, Z.I., 1994: The step-mountain Eta coordinate model: Further development of the convection, viscous sublayer and turbulent closure schemes. *Mon. Weather Rev. 122*, 927–945.

Jericevic, A., Kraljevic, L., Grisogono, B., Fagerli, H., and *Vecenaj, Z.,* 2010: Parameterization of vertical diffusion and the atmospheric boundary layer height determination in the EMEP model. *Atmos. Chem. Phy. 10*, 341–364.

Lenschow, D.H., Li, X.S., and *Zhu, C.J.,* 1988: Stably stratified boundary layer over the Great Plains. Part I: Mean and turbulent structure. *Bound.-Layer Meteor. 42*, 95–121.

Lenschow, S., and *Tsyro, S.,* 2000: Meteorological input data for EMEP/MSC-W air pollution models. EMEP MSC-W Note 2/2000.

Louis, J., 1979: A parametric model of vertical eddy fluxes in the atmosphere. *Bound.-Layer Meteor. 17*, 187–202.

Mellor, G.L., and *Yamada, T.,* 1974: A hierarchy of turbulence closure models for planetary boundary layers. *J. Atmos. Sci. 31*, 1791–1806.

Mihailovic, D.T., and *Alapaty, K.,* 2007: Intercomparison of two K-schemes: local versus non-local in calculating concentrations of pollutants in chemical and air-quality models. *Environ. Model. Softw. 22*, 1685–1689

Mihailovic, D.T., Alalapaty, K., and *Sakradzija, M.,* 2008: Development of a non-local convective mixing scheme with varying upward mixing rates for use in air quality and chemical transport models. *Environ. Sci. Pollut. Res. 15*, 296–302.

Mihailovic, D.T., Alapaty, K., and *Podrascanin, Z.,* 2009: The combined non-local diffusion and mixing schemes, and calculation of in-canopy resistance for dry deposition fluxes. *Environ. Sci. Pollut. Res. 16*, 144–151.

O'Brien, J.J., 1970: A note on the vertical structure of the eddy exchange coefficient in the planetary boundary layer. *J. Atmos. Sci. 27*, 1213–1215.

Pleim, J.E., and *Chang, J.S.,* 1992: A non-local closure model for vertical mixing in the convective boundary layer. *Atmos. Environ. 26A*, 965–981.

Pleim, J.E., 2007a: A combined local and nonlocal closure model for the atmospheric boundary layer. Part I: Model description and testing. *J. Appl. Meteorol. Clim. 46*, 1383–1395.

Pleim, J.E., 2007b: A combined local and non-local closure model for the atmospheric boundary layer. Part 2: Application and evaluation in a mesoscale model, *J. Appl. Meteor. Clim. 46*, 1396–1409.

Simpson, D., Fagerli, H., Jonson, J.E., Tsyro, S., Wind, P., and *Tuovinen, J.-P.,* 2003: Transboundary acidification and eutrophication and ground level ozone in Europe: Unified EMEP Model Description, EMEP Status Report 1/2003 Part I, EMEP/MSC-W Report, The Norwegian Meteorological Institute, Oslo.

Stull, R.B., 1984: Transilient turbulence theory. Part I: The concept of eddy mixing across finite distances. *J. Atmos. Sci. 41*, 3351–3367.

Topçu, S., Incecik, S., and *Atimtay, A.T.,* 2002: Chemical composition of rainwater at EMEP station in Ankara, Turkey. *Atmos. Res. 65*, 77–92.

Zhang, D.L., and *Zheng, W.Z.,* 2004: Diurnal cycles of surface winds and temperatures as simulated by five boundary layer parameterizations. *J. Appl. Meteor. 43*, 157–169.

Zhang, C., Randall, D.A., Moeng, C.-H., Branson, M., Moyer, M., and *Wang, Q.,* 1996: A surface parameterization based on vertically averaged turbulence kinetic energy. *Mon. Weather Rev. 124*, 2521–2536.